Studies about the influence of turbulence on the sound propagation in the atmosphere and its simulation

Florian Rost, Astrid Ziemann and Armin Raabe

Summary

Noise is still an unsolved problem of our time and influences the public health and well-being. So sound-exposure gains more and more in importance. This study examines the influence of turbulent vertical profiles of wind and temperature on the sound propagation, using the model SMART (**s**ound propagation **m**odel of the **a**tmosphere using **r**ay-**t**racing). For several states of atmospheric stability, ten-minute-time series of vertical wind and temperature profiles were constructed and used as input data for the model. Simulations of the sound attenuation showed that turbulence affects the sound propagation in the atmosphere. This influence is reflected in a reduction of the sound attenuation level in the downwind area, whereas the sound shadow remains almost unaffected. The influence increases with the distance to the source and depends on the atmospheric stability.
Beside the average influence due to turbulence, a "worst-case" scenario with the highest noise immission during the simulated time range was analyzed.
Based on the results of this study, a new SMART-module, taking turbulence into account by parameterizations, was developed. The developed turbulence module is an upgrade of the sound model SMART and helps to improve the sound immission forecasts, including meteorological effects.

1 Introduction

In Germany, more than 15 million people feel disturbed by noise [1]. Noise is not only unpleasant. It can cause people falling ill. For noise levels greater than 60 dB, the myocardial infarction risk increases continuously. Pear year, approx. 4000 myocardial infarction cases are attributed to the road traffic noise [2]. A very meaningful tool in environmental protection is the forecast of sound immission. At the *Leipziger Institut für Meteorologie* a sound propagation model, SMART (**s**ound propagation **m**odel of the **a**tmosphere using **r**ay-**t**racing), was developed [3]. In contrast to the idea that sound propagates in form of waves, this model deals with the estimation of sound energy propagation by sound rays. This is the basic principle of the geometrical acoustics [4], which is the foundation of SMART. This model computes the sound attenuation level, taking into account meteorological influences on the sound propagation by vertical profiles of wind velocity, wind direction and temperature.
In previous simulations only stationary profiles were considered. In the lowest 1 to 2 km of the atmosphere (the atmospheric boundary layer) wind shear and solar heating of the ground produce turbulent fluctuations of the vertical profiles. These fluctuations lead to sound scattering that influences the sound attenuation level [4], [5].

For this work, vertical profiles of wind and temperature including turbulent fluctuations were constructed for several cases of atmospheric stability and jointed to time series. The sound propagation for each time series were averaged arithmetically to estimate the effects of turbulence on the sound attenuation.

2 Meteorological effects on the sound propagation

The adiabatic sound speed is a function of the air temperature T. The propagation velocity of the sound also depends on the wind vector. Therefore, there the effective sound speed [4] is introduced as

$$c_{eff}(z) = c(z) + u(z), \qquad (1)$$

with the adiabatic sound speed c and the wind velocity component u along the propagation direction of the sound. A vertical increase of temperature or wind velocity leads to a vertical increase of the effective sound speed and a downward refraction of the sound ray. A vertical decrease of c_{eff} causes an upward refraction.

The sound propagation model SMART uses these properties for calculating the sound attenuation level. It is introduced in the following section.

3 The sound propagation model SMART

In the model SMART a sound source emits a number of sound rays into the atmosphere, which is regarded as horizontal homogeneous. The computation of the sound path is based on the special refraction law for a moving medium [6]. Meteorological effects on the refraction are considered by vertical profiles of wind velocity, wind direction and temperature. After the ray tracing, between two sound rays with only a small difference in the emission angle a sound tube is constructed. The cross-section of such a tube is inversely proportional to the sound intensity I. The ratio of these cross-sections at a sampling point i and at a reference distance from the source (here: 1 m) leads to the change in the sound intensity level, called sound attenuation level [3], [7]:

$$\Delta L_I = -10 \cdot \lg \frac{I_i}{I_{ref}}. \qquad (2)$$

These calculations are made for 36 horizontal directions with an azimuth angle resolution of 10 deg. Therefore the output of SMART involves a horizontal sound attenuation field. The immission level was set to a height of 2 m above ground.
The model input data include vertical profiles of temperature, wind speed and wind direction. These profiles can be taken from measurements or – as in this study – can be constructed synthetically.

3 Synthetical construction of vertical turbulent wind and temperature profiles

In a first step, undisturbed profiles were simulated. The wind profiles are based on the logarithmic wind law

$$\bar{u}(z) = \frac{u_*}{\kappa} \ln \frac{z}{z_0}, \qquad (3)$$

with the mean wind speed $\bar{u}$, height over the ground z, the *von Kármán*-constant κ ($\kappa = 0.4$) and the friction velocity u_* [8]. The roughness length z_0 was taken for $z_0 = 0.01$ m, which is an adequate value for grassland [9], was used. To take into account atmospheric stability, u_* is calculated for several stability classes, borrowed from the *Pasquill*-stability classes [10]: *Very unstable*, *unstable*, *neutral to light unstable*, *neutral to light stable*, *stable* and *very stable*. This classification is based on the *Obukhov*-length L, an stability parameter which refers to the ratio of the flux of momentum and the sensible heat flux. Profiles were constructed for the following values of L (unit: m): -10; -30; -50; -100; -200; -300; 500; 250; 150; 60; 7.

The creation of vertical temperature profiles rests upon the gradient-*Richardson*-number

$$R_i = \frac{g}{\bar{T}} \cdot \frac{\frac{\partial \bar{\Theta}}{\partial z}}{\left(\frac{\partial \bar{u}}{\partial z}\right)^2}, \qquad (4)$$

with the acceleration due to gravity g and the parameterizations $R_i = \frac{z}{L \cdot \varphi_M}$ for a stably and $R_i = \frac{z}{L}$ for an unstably stratified atmosphere [11]. Θ is the potential temperature and $\bar{T}$ the layer-average temperature. φ_M represents a stability depending function.

In the real atmosphere, such simple profiles are disturbed by turbulent eddies. A turbulent flow contains a number of eddies on different scales. The largest of them gain turbulent kinetic energy from the main airstream. These large eddies transfer their energy – without any loss of energy – to smaller ones, which convey energy by the same way. The smallest eddies with dimensions depending on the viscosity of the medium are dissipating the mechanic energy into heat. The range of energy transfer (inertial subrange) in this energy spectrum was described by *Kolmogorov* (1941) by the relation

$$E(f) \propto f^{-5/3}, \qquad (5)$$

where f is the frequency [12]. Within simulated profiles, atmospheric turbulence was included by considering the mixing length theory of *Prandtl* [11]. By a vertical impulse, an air parcel with its specific properties $\bar{u}(z)$ and $\bar{\Theta}(z)$ is mixed into a higher (or lower) altitude $(z+l)$, retaining its properties. The observation of this particle in the level $(z+l)$ is $u = u(z) = \bar{u}(z+l) + u'$. $\bar{u}$ can be seen as average wind speed and

u' as turbulent fluctuation. These relations can also be considered for Θ. The mixing length is calculated by

$$l = \kappa z / \varphi_{M,H} . \qquad (6)$$

There are several parameterizations for $\varphi_{M,H}$, according to $u(\varphi_M)$ and Θ (φ_H) [11]. They are all based on the *Obukhov*-length L.

In a fixed height over ground (in this special case 0.25 m) the mixing length is calculated and added to this height. The result is saved as a first interim stage. To the values of $\bar{u}$, $\bar{\Theta}$ or $\bar{\vartheta}$ at this height, a turbulent fluctuation u' respectively Θ' or ϑ' is added (ϑ: wind direction). For the altitude of the first interim stage, the mixing way length is calculated and added to this height. This leads to a new interim stage. This procedure is repeated until the maximum height of the model is reached.
Such profiles are constructed over a time range of 10 minutes [13]. A time series $u(z,t) = \bar{u}(z) + u'(z,t)$, $\Theta(z,t) = \bar{\Theta}(z) + \Theta'(z,t)$ and $\vartheta(z,t) = \bar{\vartheta}(z) + \vartheta'(z,t)$ is created for each interim stage.
The time- and height-dependent turbulent fluctuations u', Θ' and ϑ' are simulated in the following way:
A series of random data points is produced and assigned to a discrete time t_i, while $\Delta t = t_i - t_{i-1} =$ 0.5 s. The energy spectrum [14] of this time series has the form $E(f) \propto f^0$. After a modification, the energy spectrum becomes a *Kolmogorov* spectrum with $E(f) \propto f^{-5/3}$.
The result of a re-transformation is a time series with the typical characteristics of the inertial subrange. The adaptation of the amplitude by a scaling factor does not influence the energy spectrum.
The amplitudes of the fluctuations depend on the altitude and the atmospheric stability and are calculated according to the turbulence characteristics given by *Foken* [10] and *Thomas et. al* [15]. Examples of such profiles are shown in figure 1.

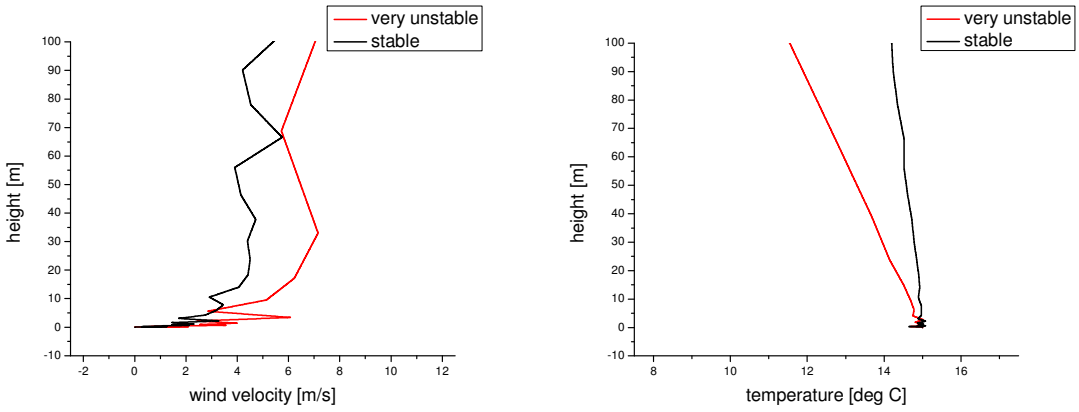

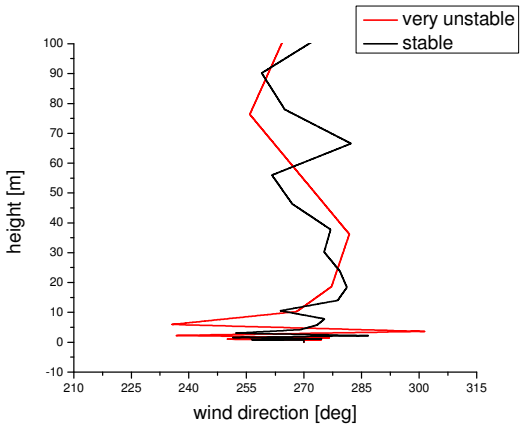

Figure 1: Examples of synthetically constructed vertical profiles of the quantities wind velocity, temperature and wind direction (from left to right). Red curves: *very unstable* case. Black curves: *stable* case.

In a next step, based on the constructed profile-time series the sound attenuation level was calculated by SMART. After first sensitivity studies about the influence of the single properties wind velocity, wind direction and temperature, profiles of all properties were combined. The sound attenuation was calculated for each selected value of the *Obukhov*-length L and arithmetically averaged over the simulated 10 minute time range.

4 Results of the SMART simulations

Figure 2 shows the sound attenuation calculated by SMART based on an undisturbed wind profile (left) and the attenuation field, averaged over the simulated ten-minute-range (right).

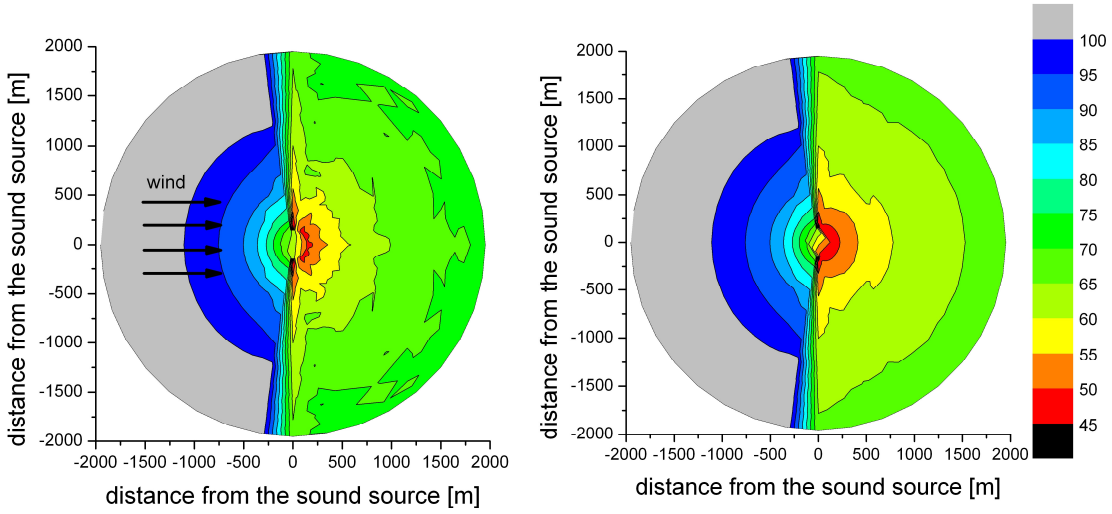

Figure 2: Sound attenuation level [dB] calculated by SMART for an undisturbed wind velocity profile (left) and averaged over a ten-minute time series of turbulent wind velocity profiles for a *very unstably* stratified atmosphere (L = -10 m) (right).

The sound source is located in the center of the circle area, right over the ground whereas the immission level lies at 2 m height above ground. Both attenuation fields are based on a *very unstable* atmosphere (stability class A, *Obukhov*-length $L = -10$ m) and a vertical wind gradient is taken into account. In the upwind area, the upward refraction of the sound rays makes no sound rays penetrating this region. This area is called *sound shadow*. In natural surroundings, diffracted and scattered sound reaches this region, hence there is no absolute silence. Referring to *Salomons* [14] SMART takes the energy conservation on the surface of a sound wave into account. With growing distance from the sound source, the wave surface is getting taller. The resulting decrease of energy density per unit of area leads to an attenuation of 6 dB per doubled distance from the source (spherical wave divergence). Additionally to this values SMART adds a constant attenuation of 40 dB [4].
It comes out that the sound shadow region is not influenced by turbulence. In the downwind area, there seems to be a decrease of the sound attenuation by the influence of turbulence. A comparison between the averaged turbulent attenuation field and the attenuation without any turbulence approves this first finding (see figure 3). To find out how strong the influence of the turbulence is for every point of the analyzed area, the attenuation field without the influence of turbulence was subtracted from the attenuation field containing turbulence. The result is the additional attenuation due to turbulence.

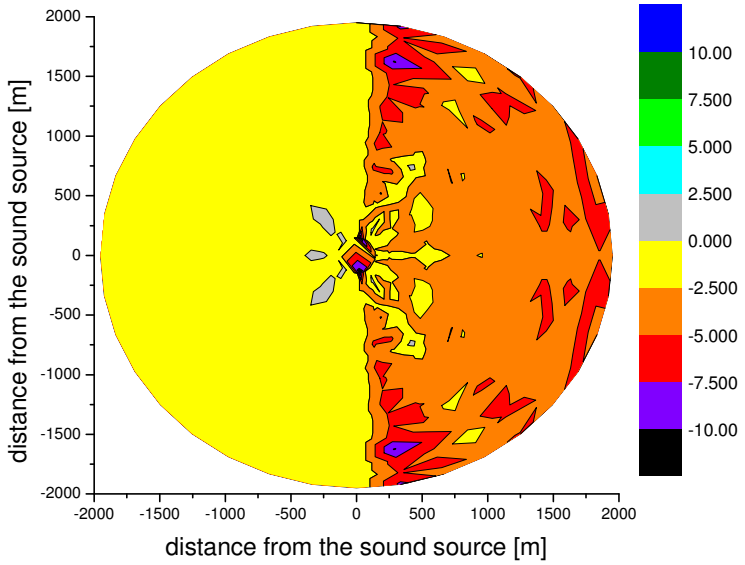

Figure 3: Additional sound attenuation [dB] caused by turbulence averaged over a ten minute time series of turbulent wind velocity profiles in a *very unstable* atmosphere ($L = -10$ m).

Similar considerations were made for vertical profiles of the temperature without wind vector influence. In this case, the effects of turbulence strongly depend on the algebraic sign of the temperature gradient, as figure 4 shows.

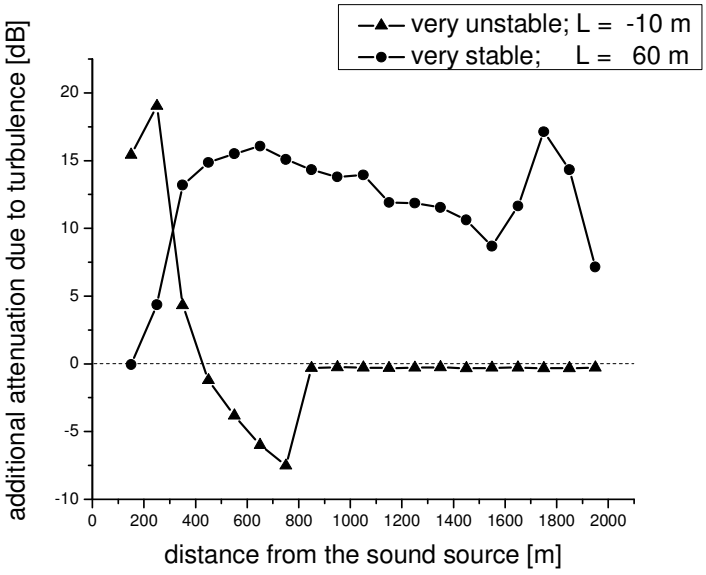

Figure 4: Additional sound attenuation [dB] caused by turbulence averaged over a ten-minute-time series of turbulent temperature profiles in a *very unstable* ($L = -10$ m) and a *very stable* atmosphere ($L = 60$ m).

The curves show the additional sound attenuation level caused by turbulence in the case of a vertical temperature decrease (*very unstable* case) and a vertical temperature increase (*very stable* case), respectively. As can be seen, there is an additional attenuation for almost all distances in the *very stable* case. In the *very unstable* case, there is an additional attenuation due to turbulence only for small distances from the sound source. For larger distances, because of the developing sound shadow no turbulence influence can be observed.

In the atmosphere wind gradients are common as well as temperature gradients. So the next step combines these profiles and uses them as new input data for SMART.

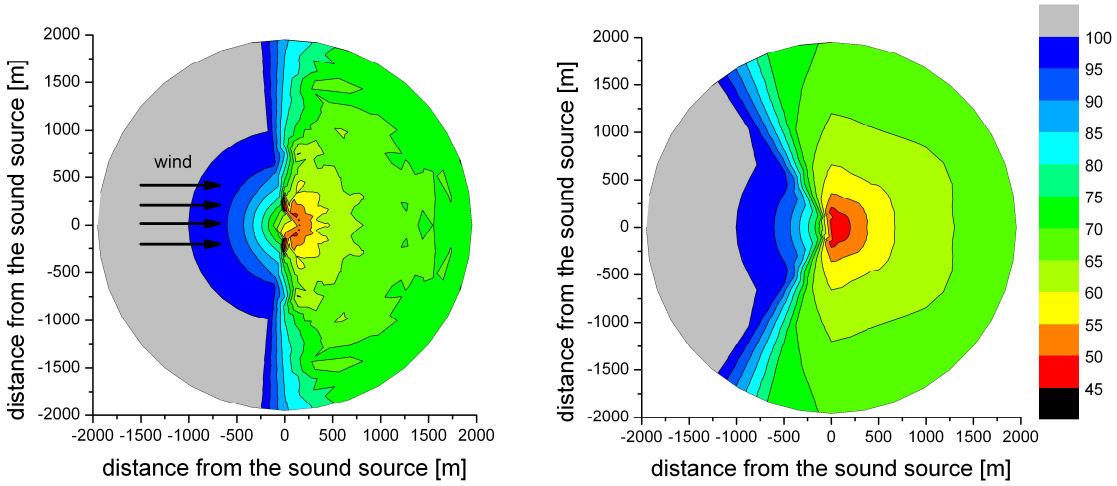

Figure 5: Sound attenuation level [dB] calculated by SMART for undisturbed combined wind and temperature profiles (left) and averaged over a ten-minute-time series of turbulent wind and temperature profiles (right) for a *very unstable* atmosphere ($L = -10$ m).

Figure 5 displays the results of these calculations. The picture on the left side was simulated with undisturbed wind and temperature profiles. On the right side, the averaged attenuation over 10 minutes with turbulent fluctuations of wind velocity, wind direction and temperature can be seen. Beside a smoothed map because of the averaging procedure, the picture of the turbulent case shows a reduced sound attenuation in the downwind area. Furthermore, the region of the sound shadow is smaller, attributed to turbulent fluctuations of the wind direction.
Among the studied stability classes, the curves of attenuation caused by turbulence have similar structures. Therefore all calculations for the same stability class (but based on different values of the *Obukhov*-length, see above) are summarized by averaging them. Figures 6 and 7 give information about the stability classes *very unstable* and *very stable*. Both of the illustrations show exemplarily two of 36 sound directions: downwind and 30 deg crosswind to downwind.

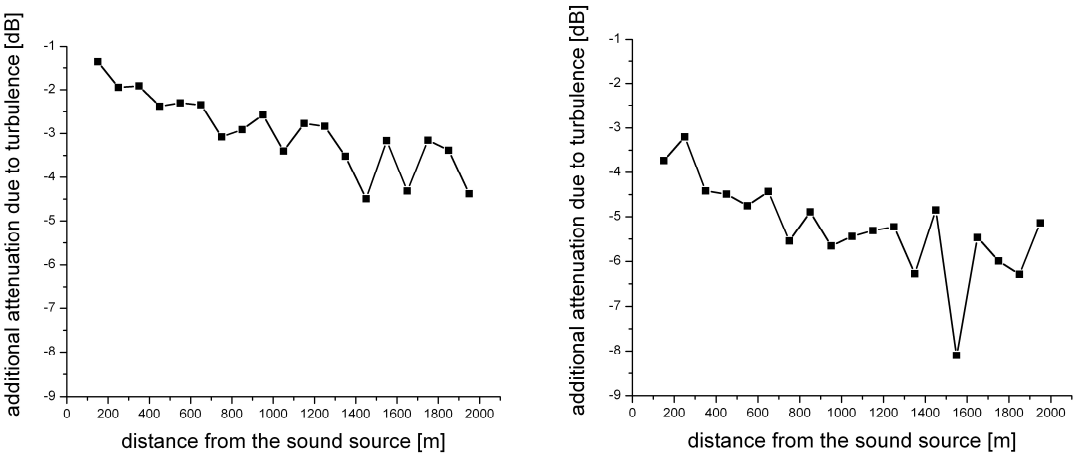

Figure 6: Additional sound attenuation [dB] caused by turbulence averaged over a ten minute time series of combined turbulent profiles of wind vector and temperature in a *very unstable* atmosphere. Left: downwind, right: 30 deg cross-wind to downwind.

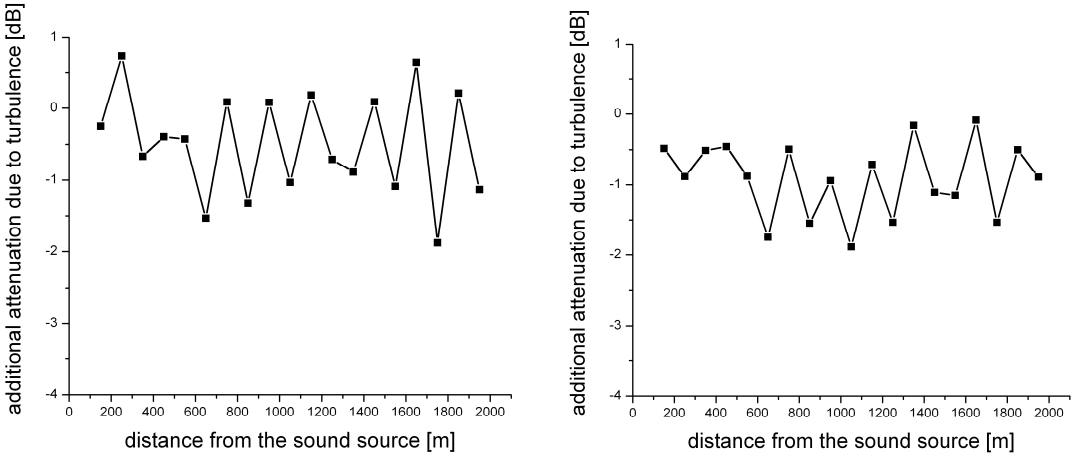

Figure 7: Additional sound attenuation [dB] caused by turbulence averaged over a ten minute time series of combined turbulent profiles of wind vector and temperature in a *very stable* atmosphere. Left: downwind, right: 30 deg cross-wind to downwind.

It comes up that turbulence leads to a decrease of sound attenuation in the *very unstable* case. This behavior amplifies with growing distance from the sound source because of the longer sound path through the turbulent atmosphere. Due to turbulent fluctuations of the wind direction, the influence in the crosswind area is larger than in the downwind direction (see figure 6).
The case of a *very stable* atmosphere shows a significant lower influence of turbulence and nearly no variation with growing distance (see figure 7).

5 "Worst case" scenarios

Beside the average additional attenuation, especially regarding noise protection, the maximal additional sound input caused by turbulence is of interest. This "worst case" selects the lowest sound attenuation values for each point of the attenuation field over the complete time range. The additional attenuation due to turbulence for this case in an *unstable* atmosphere is shown in figure 8.

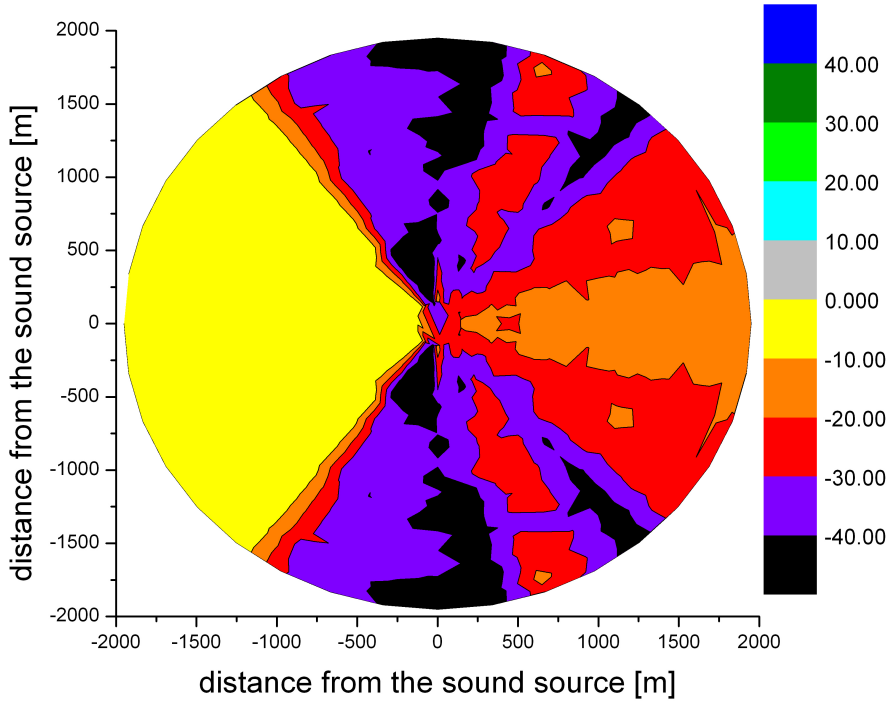

Figure 8: Minimal additional sound attenuation [dB] due to turbulence averaged over a ten-minute-time series of combined turbulent profiles of wind vector and temperature in an *unstable* atmosphere.

It can be seen that the maximal reduction of the sound attenuation caused by turbulence lies between 10 and 20 dB in the downwind direction and between 30 and 40 dB in the crosswind sections. Identical studies about a *very stable* stratified atmosphere showed a weaker influence of turbulence. There is an attenuation reduction of less than 10 dB in the downwind direction and less than 30 dB in the crosswind sections.

6 Development of a turbulence-module for the sound propagation model SMART

Based on the presented work, a supplementary module for the sound propagation model SMART was developed. The additional sound attenuation due to turbulence dependent on the distance to the sound source was parameterized by regressions of their determined values in the prefixed case studies.
The module just deals with the region from 0 to 50 deg around the downwind direction and calculates the sound attenuation due to turbulence depending on the atmospheric

stability. The applicable input parameter is one of the introduced stability classes. An example for the simulated attenuation without and with this module shows figure 9 for a *very unstable* stratified atmosphere.

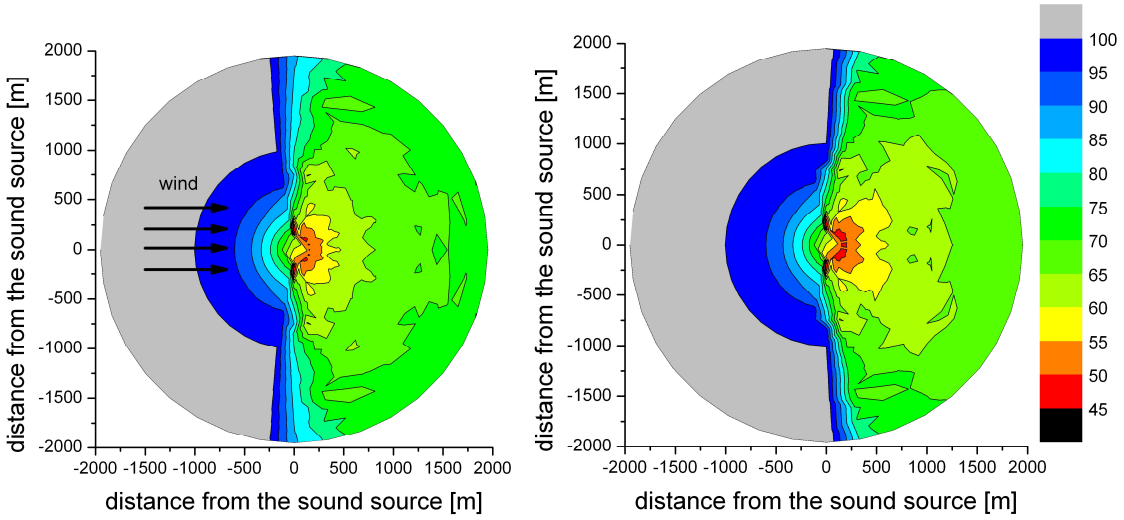

Figure 9: Sound attenuation level [dB] calculated by SMART for an undisturbed combined wind and temperature profile. Left: without any turbulence, right: including parameterized turbulence effects for a *very unstable* atmosphere.

The developed module also provides the facility to estimate the "worst case". The region is shown in grey. An example shows figure 10.

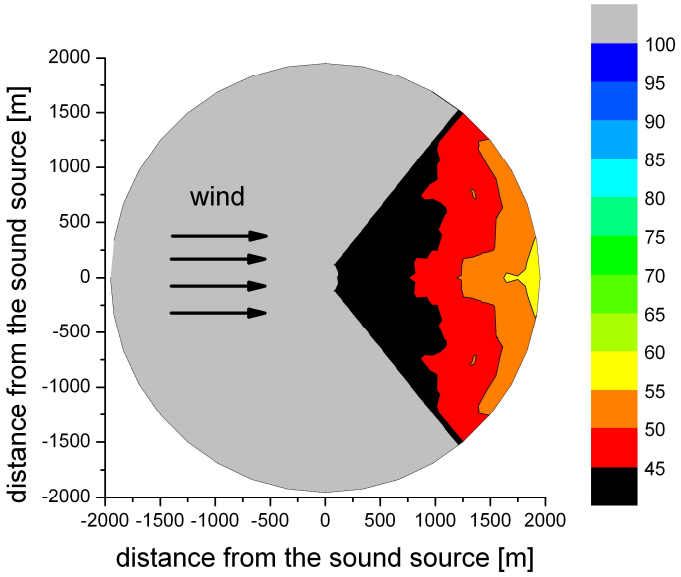

Figure 10: Minimal sound attenuation [dB] in a turbulent atmosphere calculated with the new developed turbulence module of SMART for combined profiles of wind vector and temperature in a *very unstable* atmosphere.

7 Conclusions and further prospects

The conducted studies show, that turbulent fluctuations of wind vector and temperature affect the sound propagation in the atmosphere. These fluctuations result in small-scale, local supplementary gradients in the wind and temperature profiles, which lead to a changed refraction of the sound rays.
As a result of the simulations for the stability range from *very unstable* to *stable*, turbulence causes a reduction of the sound attenuation of 2 to 8 dB in the focused area of 0 to 50 deg crosswind to the downwind direction, compared with a turbulence free atmosphere. That means in average turbulence results in a higher noise immission for a *very unstable* to *stable* atmosphere. The main influences on the initial sound shadow can be ascribed on turbulent fluctuations of the wind direction. The region 0 to 50 deg around to the upwind direction is only weakly influenced.
Furthermore it comes up, that the influence of turbulence increases with growing distance to the source. This conforms to expections, because the sound ray passes more and more turbulence elements (eddies) during its propagation through the atmosphere, so the influence of turbulence increases.
A particular position takes up the stability class *very stable*. In this case, the average additional attenuation due to turbulence in sound directions between 0 and 30 deg is neglectable. In 30 to 50 deg, turbulence leads to a reduction of the attenuation of not more than 2 or 3 dB. Furthermore, the effect of turbulence depends only weakly on the distance of the source (see figure 7). Further calculations with various profiles can also help to specify the obtained parameterizations, like simulations for other values of the *Obukhov*-length L.
As can be seen from figure 1, the strongest fluctuations of wind and temperature (and consequently the largest values of their vertical gradients) can be found close to the ground. In all simulated cases the sound source was set on the ground, so the effects near the earth surface prevail. Studies with a sound source centimeters or meters above ground verified this assumption [16] and should be continued.
A limitation of the introduced results is the fact that SMART is only able to simulate a horizontal homogeneous atmosphere. In general, this assumption is inapplicable for regarding turbulence.
The parameterization of the “worst case” scenario does not take a range of time into account, for that the sound attenuation reduction takes place. This can be modified by using another selection algorithm, which takes an immission time into account.

This study is designed to give a first idea how to consider turbulence in SMART. The new version of SMART considering turbulence is a further advance in the sound immission forecast. The option to calculate a “worst-case” scenario helps to estimate the maximal noise exposure due to meteorological effects.

References:

[1] Flasbarth, J., 2009: Lärm ist das am stärksten unterschätzte Umweltthema. Epoch Times Deutschland

[2] Babisch, W., 2006: Transportation Noise and Cardiovascular Risk. WaBoLu-Hefte 01, Umweltbundesamt

[3] Ziemann, A., 2003: Auswirkungen unterschiedlicher Schallausbreitungsmodelle auf die Lärmprognose. Wiss. Mitteil. Inst. f. Meteorol. Univ. Leipzig 30

[4] Salomons, E. M., 2001: Computational Atmospheric Acoustics. Kluwer Academic Publishers

[5] Albrecht, H.-J., Peters, E., 2007: Der Einfluss turbulenter Temperatur- und Windfluktuationen auf die Standardabweichung des akustischen Beurteilungspegels. Fachbeiträge des Landesumweltamtes Brandenburg 106

[6] Ostashev, V. E., Hohenwarter, D., Attenborough, K., Blanc-Benon, Ph., Juvé, D., Goedecke, G.H., 2001: On the refraction law for a sound ray in a moving medium. Acustica 87, p. 303 – 306

[7] Ziemann, A., Balogh, K., 2006: Gekoppelter Atmosphäre-Boden-Einfluss auf die Schallausbreitung einer höher gelegenen Schallquelle. Wiss. Mitteil. Inst. f. Meteorol. Univ. Leipzig 37

[8] Kraus, H., 2008: Grundlagen der Grenzschichtmeteorologie. Springer Berlin

[9] Zmarsly, E., Kuttler, W., Pethe, H., 2002: Meteorologisch-klimatologisches Grundwissen. Verlag Eugen Ulmer Stuttgart

[10] Foken, T., 2003: Angewandte Meteorologie. Springer Berlin

[11] Kraus, H., 2008: Grundlagen der Grenzschichtmeteorologie. Springer Berlin

[12] McComb, W.D., 1991: The Physics of Fluid Turbulence. Oxford University Press

[13] Seifert, H., 1999: VDMA Forschungsprojekt: Ermittlung von Ermüdungsdaten an großen Windenergieanlagen. DEWI Magazin 15, p. 58 – 64

[14] Press, W.H., Teukolsky, S.A., Vetterling, W.T., Flannery, B.P., 1992: Numerical Recipes in Fortran 77. Camebridge University Press

[15] Thomas. C., Foken, T., 2002: Re-evaluation of integral turbulence characteristics and their parameterizations. 15th Conference on Boundary Layer and Turbulence

[16] Rost, F., 2010: Untersuchung und Simulation des Einflusses von Turbulenz auf die Schallausbreitung in der Atmosphäre, Universität Leipzig, Institut für Meteorologie, Diplomarbeit